NASA Technical Memorandum 87131

Experimental Performance of a 1-Kilowatt Arcjet Thruster

Shigeo Nakanishi
Lewis Research Center
Cleveland, Ohio

Prepared for the
18th International Electric Propulsion Conference
cosponsored by the AIAA, DGLR, and JSASS
Alexandria, Virginia, September 30–October 2, 1985

NASA

EXPERIMENTAL PERFORMANCE OF A 1-KILOWATT ARCJET THRUSTER

Shigeo Nakanishi
National Aeronautics and Space Administration
Lewis Research Center
Cleveland, Ohio 44135

SUMMARY

A formerly unused cathode and anode/nozzle assembly from a flight model arcjet has been tested with nitrogen, hydrogen, and nitrogen-hydrogen mixture simulating ammonia decomposition products at arc power levels from about 300 to 950 W. Two different power sources and two nozzle configurations were tested at low background pressures to exclude facility effects.

Increased nozzle expansion ratio improved cold-flow nozzle efficiency from 0.8 to 0.9. Hydrogen thrust efficiency of 0.26 at 872 sec specific impulse matched some 1964 performance on a similar device. Simulated ammonia thrust efficiency was 0.31 at 422 sec.

Spontaneously occurring voltage mode changes at constant arc current could be partially stabilized with appropriate power source characteristics. In the higher voltage mode specific impulse was higher, but thrust efficiency changed only slightly from that of the lower voltage mode. Sustained tests of up to 2 hr duration exhibited no apparent performance degradation with time.

E-2744

INTRODUCTION

During the 1960's, considerable effort was expended by both the industrial and government sectors on arcjet thruster research and technology. A comprehensive survey made in 1965 documented and summarized the state of art at that time (ref. 1). Hydrogen arcjets ranging in power levels from 1 to 200 kW were investigated. Other propellants like ammonia, lithium hydride, and methane were used principally in low power thrusters.

The general conclusions at that time were: (1) arcjets operating at power levels in the tens of kilowatts were more efficient and demonstrated longer life potential than at low power; (2) electrode life was an unresolved issue although one 30-kW test ran continuously for 500 hr (ref. 2), and another test ran for 720 hr with interruptions but with a voluntary termination (ref. 3); (3) lack of sufficient space electric power and near term mission applications led to temporary abandonment of further research and development.

New space mission requirements have reawakened interest in the arcjet. As a thruster concept, it has the potential of high thrust and power densities, simplicity, and choices of propellants to suit specific impulse and system requirements.

The 1-kW arcjet used in this investigation was designed and developed by the Plasmadyne Corporation in the early 1960's as a possible candidate experiment in a space electric rocket test (ref. 4). Ground tests with hydrogen propellant demonstrated a thrust efficiency of 25 percent at a specific

impulse of 1000 sec (ref. 4). Performance degraded with time presumably due to erosion of the anode/nozzle electrode. Using ammonia as propellant, a thrust efficiency of 8 percent at a specific impulse of 550 sec was obtained. For near term auxiliary propulsion applications, ammonia and hydrazine are the favored propellants for storability reasons.

The present investigation seeks to renew and extend the testing and evaluation performed on the 1-kW Plasmadyne flight model thruster. It will establish a baseline performance of a configuration originally designed for a 24-min flight using hydrogen. As part of a continued development program, the basic components of the thruster will be tested over a range of power levels and propellant flow rates, primarily with hydrogen and a nitrogen-hydrogen mixture to simulate ammonia decomposition products. Both imposed and spontaneously occurring operational behavior will be described.

For this investigation, the basic thruster design was kept intact with only minor changes although the nozzle throat diameter increased and stabilized during the initial tests. Further changes will be motivated and guided by the understanding gained from tests on this already well-developed thruster and by design principles which evolve from these studies.

APPARATUS

Thruster

A photograph of the Plasmadyne 1-kW arcjet thruster system is shown in figure 1. In accordance with the flight test program requirements, the system size was limited to 20.3 cm in diameter, 35.6 cm length, and a mass of 5.5 kg, or less. It had to be capable of 24 min of unattended and predictable operation. The liquid hydrogen propellant tank was double-walled and vacuum jacketed. The round baffle located between the mounting bracket and the thruster nozzle was an insulated reflector shield to minimize rearward heat transfer from the radiatively cooled nozzle. Other design details are described in reference 4.

A partial cross-section view of the cathode-anode/nozzle assembly is shown in figure 2. The cathode was a 3.2 mm diameter, 2 percent thoriated tungsten rod held concentrically within a 7.8 mm o.d. molybdenum tube. Enough clearance was provided around the cathode rod to permit part of the propellant gas flow to regeneratively cool the cathode. The outside surface of the molybdenum tube had a helical groove which allowed the remainder of the propellant gas to swirl as it flowed between the tube and its boron nitride housing. The metal ring seals (K-seals) of the original design were modified to avoid propellant gas leakage which increased as repeated disassembly and reassembly progressively deformed the K-seal rings. The periphery of the sealing flange was ground to a conical surface which seated on a mating boron nitride surface. A pressure check indicated the leakage rate to be about 3×10^{-6} kg/sec of room temperature nitrogen gas at a presourse differential of 3.8×10^{5} Pa. At normal operating pressures and temperatures the leakage is estimated to be about 2.4 percent of the corresponding propellant flow rate.

The anode/nozzle configuration was originally designed for a hydrogen flow rate of 5×10^{-6} kg/sec at a nominal arc chamber pressure of 7.6×10^{5} Pa.

The tungsten nozzle insert had a throat diameter of 0.23 mm and diverged to 1.27 mm to give an area ratio of about 30. The downstream face of the nozzle was flat to benefit from any possible thrust generated by the kinetic energy of gas molecules leaving the surface. The length and outside diameter of the molybdenum nozzle was sized to accommodate radiant cooling.

For the tests at the Lewis Research Center, the cathode/anode/nozzle assembly was removed from the flight system and mounted on a thrust platform as shown in figure 3. Early tests with this installation encountered several difficulties. During high flow operation, especially with nitrogen-hydrogen mixtures, the arc plasma of the jet plume would initiate a glow discharge between the external surfaces of the anode and cathode. At other times the discharge occurred between the anode and thrust stand, anode and test facility walls, and bare electrical leads. These difficulties were minimized by; (1) electrically isolating the power system from facility ground, (2) enclosing the cathode structure in a boron nitride housing, and (3) covering all electrical leads with insulation. Inasmuch as two nozzle configurations were tested, the Plasmadyne-designed nozzle will be designated "short nozzle." As the throat diameter enlarged due to erosion, a boron nitride extension was used to provide a larger nozzle expansion ratio and to expand the nozzle contour to the outside diameter of the molybdenum body. Figure 2 shows this extension for which the nozzle coordinates were obtained from reference 5. The extension was strapped to the molybdenum body with two tantalum bands which were held in tandem but could be tightened independently. Using this approach, different nozzle configurations could be tested without altering the original anode/nozzle geometry. The second configuration with the boron nitride extension will be designated "extended nozzle."

Power System

Two types of power system were used in the investigation. The first type was the conventional dc power supply-ballast resistor combination. The 440 V, 3 phase, ac to dc power supply was rated for an output of 600 V at 20 A controllable in either voltage or current mode with automatic crossover. The manufacturer's specifications of nominal ripple content was verified to be 0.8 V plus 0.4 percent of the output voltage.

The ballast resistor consisted of four 3 Ω rheostats connected in series with a rated current of 12.9 A with continuous air cooling. Although of undetermined benefit, a 1.0 mH inductor was included in the circuit to make the series R-L-C circuit overdamped.

Most of the testing was performed with the conventional power system. Some tests were also performed with a 10 kHz pulse-width modulated solid state power processor designed and built at the Lewis Research Center (ref. 6). No ballast resistor was required and the power processor operated at greater than 90 percent efficiency.

Instrumentation

Thrust measurement. - The thrust measurement system consisted of a 12.7 by 22.9 cm platform upon which the arcjet thruster was mounted using appropriate thermal isolation. The platform itself was supported on four flexure

springs made of 1.27 by 4.3 x 0.023 cm thick machined stainless steel. The motion of the platform due to applied thrust was transmitted mechanically to a strain gage force transducer. The transducer was rated for a force of 1.47 N full scale so that the resisting force against the applied thrust was due to both the flexure springs and the force transducer. Thrust stands of the same design have been used extensively in resistojet testing (ref. 7).

The mechanical pumps of the two vacuum facilities operating in the same building, caused an unacceptable amount of vibration in the thrust platform. It was necessary to incorporate a pair of friction-free viscous dampers filled with low vapor pressure diffusion pump fluid. The signal output from the force transducer was of the order of 0.10 V with 5 V dc excitation across its strain gauge bridge. For recording on the multi-channel recorder, the output signal was filtered with an active notch filter set between 6 Hz low pass and 100 Hz high pass. The filtered signal was then fed to a variable gain differential dc amplifier so that the recorder output could be calibrated to read directly in convenient engineering units.

Calibration was performed by successively applying or removing 4 gm lead weights attached to a windlass via a monofilament thread. By using three such weights, the thrust measurement system was calibrated from 0 to 0.118 N with a recorded resolution of 4.9×10^{-4} N in the 0.049 N full scale range to 2.5×10^{-3} N in the 0.245 N full scale range. True accuracy under dynamic loading has not been established, but static error was less than ±1 percent of full scale with linearity within 0.8 percent up to 0.12 N.

The greatest difficulty encountered was drift of the zero point during long tests because of thermal input to the thrust measurement system. As mentioned previously, the thruster was mounted on the thrust platform using two thermally isolated mounts. The aluminum base of the thrust stand was water-cooled with a copper coil imbedded in a milled groove. In addition, a water cooled copper enclosure was placed over the entire thrust stand with only the thermally isolated thruster mounts protruding. During long tests of 1 hr or more a small zero drift was still present, but thrust zero was established periodically by a method described under Procedure. In-situ calibration during thruster operation was performed to verify the load increment accuracy of thrust measurement in spite of the zero point drift.

Power metering. - Arc power was obtained by measuring the arcjet voltage and current at the electrical feed-through terminals outside the vacuum facility. The current sensor was a calibrated shunt rated for 100 mV output at 20 A in the line to the cathode. The output signal was amplified through a differential input dc amplifier before going to a signal isolation system. The arc voltage signal was divided to a suitable level before isolation.

In order to operate the arcjet electrically isolated from facility ground without exceeding the common mode isolation limit of the multi-channel recorder, the arc voltage and current signals were sent to a pair of transformer-coupled isolation amplifiers. The entire system was calibrated by applying known signals at the feed-through terminals.

Flow metering. - The flow control and metering system was designed to use selectively gases such as argon, nitrogen, hydrogen, and nitrogen-hydrogen

mixtures. Three separate gas inlet lines were cross-connected and valved with bellows-sealed shut off valves to eliminate leakage.

The flow meters were commercially available thermal conductivity element type with a full scale indicated range of 5000 stdcm^3 with full scale accuracy of 1 percent. Periodic flow calibration of the flow meters was performed in-situ by measuring the time rate of pressure change into a known volume. Flow adjustment was performed with a micrometer screw type leak valve, also with bellow seals. A final valve after the flow adjustment and mixing points conveniently allowed shut-off and turn-on without readjustment of the flow rates of a single gas or mixture of gases.

Arcjet chamber pressure measurement was limited to the gas feed line pressure at the vacuum feed-through flange. The pressure drop in the feed line between the point of measurement and the arcjet was determined by measuring the feed line pressure as a function of flow rate with the line disconnected at the arcjet and exhausting to atmosphere. The maximum pressure drop was about 2.9×10^4 Pa at 5000 stdcm^3 of nitrogen, and much less for other gases.

Data recording. - Simultaneous recording of up to eight variables was accomplished by means of a multi-channel direct inking strip chart recorder. Each channel had fixed gain or variable gain adjustments and chart speeds up to 200 mm/sec. For most of the arcjet operation a recording speed of 1 mm/sec was used. The following table shows the recorded variables and their full scale readings.

Channel	Variable	Full scale
1	Thrust transducer, °C	0 to 50
2	Thrust, N (selectable ranges)	0 to 0.049
		0 to 0.098
		0 to 0.245
		up to 1.47
3	Nitrogen (Argon) flow, stdcm^3	0 to 5000
4	Hydrogen flow, stdcm^3	0 to 5000
5	Feed line pressure, psia (selectable)	0 to 50
		0 to 100
6	Arc voltage,	
	low range, V	0 to 100
	high range, V	0 to 200
7	Arc current, A	0 to 20
8	Bell jar pressure, torr (decade)	0 to 10×10^{-3} to 10^{-7}

Vacuum Facility

The vacuum facility used for the tests was a 1.5 by 5 m long chamber with four 82 cm diameter oil diffusion pumps and a rotary blower backed by a mechanical roughing pump. The rated pumping capacity of each diffusion pump was 15 000 liters/min at 10^{-4} torr. For convenience and economy, tap water was used in the diffusion pump cold traps instead of liquid nitrogen.

As shown in figure 3, the thruster was installed in a 0.9 m diameter by 0.8 m cylindrical test section which could be isolated from the vacuum facility

by closing a 0.9 m diameter gate valve. Actual pumping performance in the test section was about 3×10^{-4} torr at a nitrogen flow rate of 19.7×10^{-6} kg/sec and 5×10^{-3} torr at 99×10^{-6} kg/sec. Thrust measurements were restricted to thruster operation with test section pressures no greater than 1×10^{-3} torr to minimize its effects on nozzle performance. The effects of background pressure were determined for each nozzle configuration by measuring the thrust from a constant flow rate of room temperature gas while varying test facility pressure.

PROCEDURE

Test procedure included those which were routinely followed regardless of test type and others which were specific to a given test. Prior to any test, after temperature equilibrium was obtained, the thrust measurement system was calibrated. The signal output with each calibration weight was recorded on the strip chart to perform a total system calibration. With the arcjet at room temperature, a cold-flow (room temperature gas) calibration was then performed for each gas or mixture of gases over the flow range normally used in thruster operation. Recorded variables for cold flow were thrust, gas flow rates, feed-line pressure, and bell jar pressure.

The arcjet was ignited by throttling the final shut-off valve in the flow metering system causing the pressure in the arc chamber to drop. At whatever pressure was required for a Pasehen breakdown with an applied 400 to 600 V, the arc current would suddenly jump to the controlled value set in the power supply output. The shut-off valve was then immediately opened to obtain the pre-set gas flow rate and steady arc operation at the selected arc current.

Accurate performance measurements required several minutes of steady-state operation to obtain equilibrium conditions depending upon the type of input variable change. This introduced the possibilities of long-term thermal drift in the thrust system zero reading. Particularly in long tests, it was necessary to reestablish the zero point periodically by shutting off the arc and the gas flow to obtain a known zero thrust condition.

RESULTS AND DISCUSSION

The initial part of this section will discuss arcjet operation and characteristics which were common to both nozzle configurations tested. Included in the discussion are the voltage-current characteristics of the arc and typical load lines for the two types of power sources used to operate the arcjet.

In order to characterize nozzle performance apart from arc operation, the short and extended nozzle configurations were tested under cold flow conditions. Operational arcjet, or hot flow, performance of the two configurations are then presented. Finally, the improved performance obtained with the extended nozzle configuration in a sustained test with a nitrogen-hydrogen mixture will be shown.

The terms and definitions used throughout the report are given in appendix A.

Operational Characteristics

With initial short runs of familiarization, the arcjet could be started and operated reliably. Each post-run examination showed the nozzle throat to be eroding more rapidly than anticipated. Within an accumulated run time of less than 1 hr, the originally 0.23 mm diameter nozzle throat enlarged to 0.76 mm. The throat diameter stabilized at the latter value, and all performance data reported herein were obtained with the larger throat. Periodic gage measurements showed no apparent increase in throat diameter except for noncircular irregularities visible in the photomicrograph shown in figure 4. These irregularities did not change appreciably with accumulated run time which was in excess of 20 hr at the time of the photograph. A further enlargement of the photograph was used to determine the cross-sectional area, which was found to be 4.623×10^{-7} m^2, or 1.4 percent greater than the circular area of a 0.76 mm diameter hole. Also visible in the photograph are small globules of molten metal which are believed to be from the throat and nozzle wall immediately downstream of the minimum area section where the arc struck. The nozzle throat region was almost always white hot, and anode melting was probable during operation with the arc seated in this vicinity.

Component tests have been conducted on constricted arcs and their results are reported in companion papers. Mass loss in radiation-cooled anodes was found to decrease with increased gas flow rate (ref. 8). In vortex-stabilized constricted arcs with water cooled anodes, erosion was found to be minimal (ref. 9). These results tend to indicate that the constrictor and nozzle throat are regions of extremely high temperatures which must be controlled or limited to minimize erosion.

Starting. - As mentioned in Procedure, the arcjet was usually ignited by initiating a low pressure gaseous breakdown. It was also possible to start at full gas pressure by moving the cathode to draw an arc, or sometimes simply by applying 400 V to the anode.

Startup was usually easy and smooth with argon, while hydrogen and nitrogen-hydrogen mixtures were often harder to start. In extreme cases, when voltages up to 600 V were required, a less stressful method of starting with argon and changing over to other gases was used. No clear reason for difficult starting has been identified, and definitive tests are better reserved for a final configuration in which performance and life requirements have also been integrated into the design.

Mode change instability. - At least two major recognizable modes of arcjet operation have been observed. While the arc current and all other parameters such as propelled flow rate and background pressure were held constant, the arc voltage was observed to shift from a low to higher voltage mode, operate in that mode for a period of time and then drop back to the lower voltage mode. These mode changes were accompanied by the appearance or disappearance of a visible plume downstream of the nozzle. The plume was highly visible in argon when operating in the high voltage mode. With H_2 and N_2-H_2 mixtures, the plume was much less luminous but still visible under subdued lighting conditions. In the low voltage mode, the plume would disappear although a bright discharge was still visible upstream of the nozzle throat. Observations indicated that the low voltage mode corresponded to anode arc attachment upstream of the nozzle throat and downstream attachment in the

higher voltage mode. The flow region downstream of the throat, being a region of decreasing pressure, was also characterized by a diffuse arc attachment to the anode. Later discussion will show that the mode change instability could be alleviated with proper power controller characteristics.

Voltage - Current Characteristics

The relationship between arc voltage and current is shown in figure 5. The data include two propellant gases over a range of propellant flow rates, and typical load lines for the ballasted and the pulse width modulated power sources. In all cases, the arc voltage decreased with increasing current which is characteristic of high current arcs. The curves for hydrogen show the low and high voltage modes of operation at the same propellant flow. For a given mode, the arc voltage generally increased with flow rate. The arc extinction limits for all the cases shown were between 4 and 5 A regardless of arc power which varied from about 269 to 600 W before extinction depending upon voltage mode and propellant type.

The arc characteristics with the nitrogen-hydrogen mixture, when operated with the modulated power source, were also examined. The controllable current range was narrow because of the output characteristics of the modulated source. The voltage-current characteristics of the arc were found to be similar for both power sources when operating in the same arc voltage mode.

Superimposed on the arc characteristics are the output load characteristics of the two power sources. The higher ballast resistance resulted in a steeper load line but also in higher power dissipation.

The pulse width modulated power source improved the arc current regulation without incurring the large power dissipation. Its output characteristics for a range of load resistance at a fixed current control setting are shown in figure 5. Other values of current setting would generate a family of curves displaced to either side of the one shown. The steepness of the output curve implies a very tight current regulation and should be helpful in maintaining constant arc current during rapid changes in effective arc resistance.

The changes in arc voltage mode are believed to be associated with movements of the attachment point and corresponding changes in arc voltage drop. Sometimes the mode change could be intentionally produced by changes in gas flow rate, arc current, or both. At other times, the mode change could occur spontaneously with no perceptible change in the externally controlled operating parameters. An example of arcjet behavior with the two types of power source is shown in figure 6. Reproductions of the strip chart recording of the various signals are shown with their nomenclature and full scale values.

Figure 6(a) illustrates an arcjet mode change from 76 to 52 V while operated with a ballasted power source at 10 A arc current using hydrogen propellant. The arc current trace appeared noisy, but the very fast and large current spikes might have been EMI induced noise affecting the instrumentation. Attempts to restore the higher voltage mode by stopping and restarting were unsuccessful. A quick change to the modulated supply and a restart obtained the quiet, higher mode operation shown in figure 6(b) at essentially the same arc voltage as with the ballasted supply. Continued operating at constant conditions began to encounter short downward excursions in voltage, but each

time the voltage returned and remained in the higher mode. It is believed that the ballasted system would have allowed drop-off into the lower mode without regaining the higher mode operation.

Thruster Performance

Because of the rapid initial erosion of the nozzle throat, meaningful performance data with hydrogen intended for the original configuration were not obtained. After the throat size stabilized, the thruster was operated with hydrogen, nitrogen, and a N_2 + 3 H_2 mixture simulating ammonia decomposition products.

Cold flow. - Cold flow data with room temperature gases were obtained with each configuration to evaluate nozzle performance exclusive of heat addition and unknown gas composition effects. These effects undoubtedly change nozzle performance, but if the nozzle thrust coefficient is assumed nearly constant, the ratio of nozzle inlet pressures between hot and cold flow conditions, to first order, is an indication of the thrust ratio, and hence specific impulse. With the short nozzle, cold flow tests with and without the cathode were made. The purpose for removing the cathode was to obtain nozzle performance without the large internal pressure drop and the possible effects of the cathode tip located close to the nozzle throat.

Cold flow thrust measurements with different gases were found to be linear functions of mass flow rate as expected for a constant gas temperatures. The cold specific impulse for each gas was, therefore, also constant over the flow range. The theoretical specific impulse, I'_{sp}, (eq. (A1)) for each gas can be used to define nozzle efficiency as a ratio of measured to theoretical specific impulse.

The nozzle efficiency for the short nozzle with cathode, short nozzle without cathode, and extended nozzle with cathode is shown in figure 7. For all three cases, the nozzle efficiency was highest with nitrogen, intermediate with the nitrogen-hydrogen mixture, and lowest with hydrogen. Of the two pure gases for which gas properties are known, nitrogen was operating at a Reynolds number, based on the throat diameter, of 1370 to 5500. The Reynolds number in hydrogen was 400 to 1400. These values were based on gas viscocities near room temperature. At higher gas temperatures the Reynolds number would be lower. The effects of having the cathode present were relatively minor but were most noticeable with hydrogen. A more significant effect on nozzle efficiency was due to the increased expansion ratio of the extended nozzle. Comparing the short and extended nozzle configurations with cathode in place, the nozzle efficiency increased approximately 0.10 for all three gases. Using one-dimensional isentropic flow relationships, the ratio of exit velocities, hence specific impulses, of nozzles with different expansion ratios can be shown to vary inversely as the expansion ratios and inversely as the nozzle exit pressure raised to the power, 1/k, where k equals the specific heat ratio of the gas flowing at constant inlet temperature and mass rate. The exit pressure in the extended nozzle was assumed equal to the facility background pressure. In the short nozzle, the effective area over which the true exit pressure extended is not clear. Because of nozzle throat erosion, the expansion ratio was about 2.78. Neglecting the exit pressure effect upon the underexpanded nozzle exit area, the extended nozzle with an expansion ratio of 2300 could result in an exit velocity, or specific impulse, about 30 percent

greater. In practice, the specific impulse was only 10 percent greater. The effects of the flow field in the exit plane of the short nozzle are undetermined, but one-dimensional flow theory does imply the possibility of the observed increase in nozzle performance. It is interesting to note that for the extended nozzle, the nozzle exit pressure after isentropic expansion was calculated to be 3×10^{-6} times the nozzle inlet pressure. A representative inlet pressure obtained with cathode removed was 7×10^{4} Pa at a nitrogen flow rate of 60×10^{-6} kg/sec. The calculated nozzle exit pressure would be 0.21 Pa, or 1.6×10^{-3} torr. The test facility background pressure at this nitrogen flow rate was 9×10^{-4} torr as measured by an ionization gage.

The feed line pressure for each gas for the short nozzle configuration is shown in figure 8. Actually, pressure in the arc chamber just ahead of the nozzle would be of greater interest, but there was no convenient way to measure this pressure. The regenerative flow design of the cathode will be shown to cause considerable pressure drop in addition to the line drop between the point of pressure measurement and the thruster connector. The data in figure 8 show considerable departure from the linear relationship suggested by one-dimensional choked flow calculations, and a different minimum area would be inferred for each gas. The reasons for these discrepancies are not clear, but the well-behaved linearity in the thrust measurement independent of pressure indicated that a better measurement of nozzle inlet pressure was needed. In all cases, the calculated throat area was smaller than the circular area of a 0.76 mm diameter hole. To obtain a larger calculated area, the pressure should be lower, which would be the case if pressure drop occurred between the point of measurement and the nozzle inlet.

The measured pressure with the cathode removed is shown in figure 8(b). In comparison, the feed pressure without the cathode was approximately 0.5 to 0.6 of the pressure with cathode in place (fig. 8(a)). The resulting calculated throat areas were correspondingly larger but still less than the physical area.

The measured thrust and nozzle parameters for the short nozzle configuration with the cathode removed are shown in figure 9. This was the only configuration for which measured feed line pressures closely approximated nozzle inlet pressures. The measured thrust shown in figure 9(a) was linear with pressure and almost formed a single line for all gases. The pressure-thrust relationship can be expressed as, $F = C_F A^* P$, where C_F, A^*, and P are the thrust coefficient. throat area, and nozzle pressure, respectively. If the thrust coefficient were constant over the pressure range, thrust would be linear with pressure.

Dividing the measured thrust by the measured pressure yields the parameter, $C_F A^*$, shown in figure 9(b). Assuming an area of 4.56×10^{-7} m^2 for a 0.76 mm diameter throat, the thrust coefficient shown in figure 9(b) is representable by a curve that is characteristically flat at the high pressure end and droops with decreasing pressure. As an upper limit, the theoretical thrust coefficient is indicated. The value of 1.8 corresponds to a fully expanded nozzle operating at a large pressure ratio with a perfect gas having a specific heat ratio of 1.4. Departure of the asymptotic value from the ideal is believed to be due to the viscous flow effects of a small nozzle at low Reynolds number.

Hot flow. - The short nozzle configuration was tested with hydrogen and N_2 + 3 H_2 mixtures over a range of arc discharge power. The performance in terms of thrust efficiency and specific impulse is shown in figure 10. The lower bound of efficiency with hydrogen was 0.10, similar to some Plasmadyne data obtained 20 yr ago. Their test reports did not fully explain the causes of performance variations other than thrust measurement uncertainties and nozzle throat erosion of 11 to 44 percent along different diameters. A broader range of thrust efficiency was obtained at that time, the maximum being about 0.27 compared with 0.175 recently. The early specific impulse was approximately twice as high, primarily because the arc power level was more than double that of recent tests. Based on input power and mass flow rate, the specific energy input for the Plasmadyne data was about 2.5×10^8 J/kg compared with about 7×10^7 J/kg in the recent tests.

With the N_2 + 3 H_2 mixture, the efficiency ranged from 0.07 to 0.12. A single reported value by Plasmadyne for ammonia gave a specific impulse of 550 sec at an efficiency of 0.08 for 920 W of arc power. It should be noted that the thrust efficiencies obtained with the nitrogen-hydrogen mixture have not been corrected for the dissociation energy inherent with ammonia. Unless this energy is recovered by regenerative cooling or recombination, the efficiency would be lower. The energy input for Plasmadyne's ammonia test was 1.8×10^8 J/kg compared with 3×10^7 J/kg for the nitrogen-hydrogen mixture.

Performance of the extended nozzle configuration operated in various gases and with normal and reversed polarities is shown in figure 11. Reversed polarity operation denoted by the solid symbols was obtained by reversing the external power lead connections so that the normally cathode electrode was positive with respect to the nozzle/anode. The data points cover a range of propellant flow rates and arc power. Thrust efficiency ranged between 0.15 to 0.30 over a specific impulse range of 200 to 900 sec. Maximum efficiency and specific impulse obtained with hydrogen were 0.26 at 872 sec; with nitrogen, 0.23 at 220 sec; and with the nitrogen-hydrogen mixture, 0.31 at 422 sec.

The reversed polarity operation gave slightly higher efficiency with hydrogen at the high end of the I_{sp} range. Within the scatter of the data, however, neither polarity showed a clear superiority.

The thrust to power ratio shown in figure 11(b) varied from about 0.22 to 0.05 N/kW, decreasing with increasing specific impulse for propellants with lower molecular weights.

Nitrogen-Hydrogen Mixture Test

Previous tests had been run at essentially constant propellant flow rates. These tests were made with the ballasted power supply, and changes in thruster operation included both intentional and spontaneous variations in arc power.

Two separate tests of different duration using a 1:3 mixture of nitrogen and hydrogen were made with the pulse width modulated power processor at essentially constant current. The processor tended to maintain the higher voltage mode operation more consistently, although short periods of the lower mode operation did occur. Intentional periodic shutdowns were also included to re-establish the thrust stand zero.

A time plot of a 2-hr test is shown in figure 12. The total run time had three phases shown by data points interconnected by dotted lines to indicate the sequence, not to infer a functional relationship with time.

The first phase was a startup and stabilizing period during which the arc current was controlled to a mean value of 8 A with a random variation of ±0.4 A. The arc voltage fluctuated ±10 V about a mean value of 80 V. At 20.7 min into the test, the arc spontaneously became quiet and stable at 92 V and 8.8 A.

The second phase of the test was at essentially constant power with a shutdown and thrust zero reading at 33, 63, and 91 min into the test. Several spontaneous changes to the lower voltage mode occurred during this phase. The first change occurred 29.3 min into the test with the arc voltage dropping to 74 V at 9 A. The arc persisted in this mode for 3 min at which time the propellant flow rate was increased to 31×10^{-6} kg/sec. The increased flow rate helped the arc to resume the high voltage mode at 86 V and 10 A.

Following the first intentional shutdown and restart, the arc remained in the low mode for 36 sec before transition to the high mode. It sustained [illegible] mode continuously for 26 min until a low mode change lasting 40 sec occurred then regained the high mode before shutdown at 63 min. The second run began in the low voltage mode which persisted for 3 min before transition to the high mode. Prior to the third shutdown at 92 min into test, one mode change occurred which lasted about 2 min before returning to high mode.

The final test phase lasting 30 min was at various propellant flow rates and nearly constant arc current of 9.2 to 10 A.

The range of $N_2 + 3\ H_2$ propellant flow rate is shown in figure 12(a). The flow rate was increased slightly for the second phase of the test and the variations that occurred during that period were due to drift. The final phase of the test took the flow rate to a maximum value allowable while maintaining the test facility pressure in the low 10^{-3} torr ranges. Allowing sufficient time for the flow and thruster operation to stabilize, the flow rate was incrementally reduced until the arc became fluctuating and unstable.

The variations in arc power shown in figure 12(b) were due to variations in arc voltage because the current was essentially constant. Increased flow tended to increase the arc voltage provided the arc remained in the high voltage mode. This trend was especially noticeable in the third phase when a decreasing propellant flow rate caused a lowering of the arc voltage, hence arc power.

The specific impulse shown in figure 12(c) reached 400 sec and held constant for most of the second phase. The initial increase in I_{sp} occurred when the arc power was increased from 264 to 666 W. The corresponding increase in I_{sp} from 210 to 314 sec resulted in a 50 percent increase in I_{sp} for a 152-percent increase in power.

The second jump in specific impulse was 20 percent for a 26.5 percent increase in power with a noticeable increase in efficiency, (fig. 12(d)).

During the third phase of the test, the specific impulse was essentially constant despite a reduction in arc power. The propellant flow rate was being reduced, and the constant I_{sp} indicated that the gas temperature was remaining essentially constant.

The feed line pressure during the changes in propellant flow rate varied from 19.3 to 27.6×10^4 Pa. Thermodynamic properties of ammonia at 20.3×10^4 Pa show that for an equilibrium gas temperature of 3000 K, ammonia would be almost totally dissociated, the constituent gases being primarily N_2 and H_2 with only a mole fraction of 0.01 as monoatomic hydrogen (ref. 10). The theoretical molecular weight of this mixture is 8.125. The theoretical specific impulse for this mixture is 473 sec. A nozzle efficiency of 0.87 would lower the specific impulse to 411 sec, which is very nearly what was obtained experimentally. The equilibrium specific enthalpy increased from 1.4×10^7 J/kg at 3000 K to 3.75×10^7 J/kg at 4000 K. Between these two temperatures, the mole fraction of monoatomic hydrogen increases from 0.091 to 0.567. Under equilibrium flow conditions the changes in gas enthalpy should be recoverable as kinetic energy, and hence specific impulse. The fact that much less than one-half the fractional energy change in the arc manifested itself in specific impulse change indicates that the gas temperature was approaching a level wherein hydrogen dissociation increased but the energy of dissociation was lost in frozen flow. The pressure range noted above was propellant feed line pressure. The arc chamber pressure was considerably lower which would hasten the onset of hydrogen dissociation and the corresponding frozen flow losses.

The thrust efficiency obtained throughout the test is shown in figure 12(d). After operation stabilized, the efficiency was nominally 0.3 over a test time of more than an hour. During the final phase when propellant flow was reduced, the efficiency also dropped. The relatively small change in arc power of 150 W over 10 min allowed sufficient time for nozzle temperatures to stabilize from point to point as flow was decreased. With constant specific impulse, reductions in propellant mass flow would lower the efficiency as shown by equation (A3). Phenomenologically, these trends might indicate increased frozen flow losses at the lower arc chamber pressures, or poorer energy transfer to the gas and higher wall losses. At the lowest feed line pressure of 19×10^4 Pa, the nozzle thrust coefficient was believed to be in the asymptotic region, hence gas expansion was at essentially constant nozzle efficiency.

The previously described test used a slightly atypical starting sequence which might have resulted in a relatively long starting transient. A second test lasting 31 min was run to compare the transient behavior of a typical starting sequence, also using the modulated power source. Time plots of the same variables are shown in figure 13. The flow rate of nitrogen-hydrogen mixture was set at 31.07×10^{-6} kg/sec from the beginning of test as shown in figure 13(a). A momentary throttling was used initially to obtain ignition as described under Procedure and immediately brought up to rated flow. As shown in figure 13(b), the arc power soon after start was 696 W corresponding to 69.6 V at 10 A, the arc current maintained throughout the test. Approximately 2 min into the test the arc power jumped to 930 W, or 93 V at 10 A, corresponding to the high voltage arc mode.

Over the ensuing 12 min, the arc power was essentially constant. Minor variations were due to small changes in arc voltage as the arc chamber increased in temperature and gas pressure. At 14 min into the test a spontaneous change to the low mode occurred which lasted for 42 sec before reverting to the previous high mode. For the remainder of the test the arc power, hence voltage, drifted downward slightly to 900 W. Two short periods of low mode operation lasting 66 and 3 sec occurred before intentional shutdown at 32 min.

The specific impulse shown in figure 13(c) reflected the variations in power. Immediately after start, the specific impulse was about 333 sec and increased to over 400 sec with increasing arc power and with thruster temperature. The mode change caused a momentary drop but not to the starting level because of the higher arc power and temperature. At the end of the test, the specific impulse immediately after arc extinction was 283 sec which was within 20 sec of the specific impulse at the three intentional shutdowns of the previously described longer test (fig. 12). The cold gas specific impulse evaluated before start of test was 132 sec. The difference of 151 sec is attributed to gas heating from the hot wall surfaces.

The thrust efficiency variation during this short test is shown in figure 13(d). During the initial 2 min of the test before mode change, the efficiency increased from 0.21 to 0.26. At the voltage mode change, the efficiency increased to 0.27 and continued to increase as the thruster approached equilibrium operating temperatures. A slight drop in efficiency occurred when the arc dropped momentarily into the low voltage mode. Two subsequent changes to the low mode resulted in small increases in thrust efficiency. By the end of the 32 min test, the efficiency was stabilized at about 0.30.

CONCLUDING REMARKS

A nominal 1 kW arcjet thruster designed and developed by the Plasmadyne Corporation in the 1960's has been tested at the Lewis Research Center over a range of arc power from about 300 to 950 W using various propellants. The internal design of the thruster was kept essentially the same as the original. Two nozzle configurations having greatly different expansion ratios were tested. The tests established a data base of currently attainable performance and showed several aspects of arcjet operational behavior. A pulse-width modulated power source permitted controlled operation over sustained periods of time including intentional shutdown, restarts, and spontaneous transitions into and out of changes in arc voltage modes.

Thrust measurements of known and reproducible accuracy have been used to calculate thruster performance. Maximum thrust efficiency and specific impulse obtained with hydrogen were 0.26 at 872 sec; with nitrogen 0.23 at 220 sec; and with a 1:3 mixture of nitrogen and hydrogen, 0.31 at 422 sec.

The nozzle configuration with an expansion ratio of 2300 was found to obtain up to 0.9 of the theoretical specific impulse when operating with equilibrium gas at room temperature. The gas flow during arcjet operation was probably nonequilibrium, and frozen-flow and viscous losses can be expected to reduce nozzle efficiency. Test facility pressures maintained below

1×10^{-3} torr minimized background pressure effects upon the nozzle and more fully utilized the high expansion ratio.

Sustained tests of up to 2-hr duration exhibited no apparent performance degradation with time. Other issues like lifetime starting transients, and operation with propellants such as hydrazine are not clearly defined at this time. These and other issues related to a complete arcjet flight propulsion system are currently being addressed.

APPENDIX A

Arcjet Performance

The conventional symbols and equations used in evaluating arcjet performance are set forth herein for convenience with a minimum of explanatory detail.

A^* nozzle throat area, m^2

C_F thrust coefficient

F thrust, newton

g gravitational acceleration, 9.8 m/sec^2

h,c subscripts denoting hot and cold conditions

I_{sp} specific impulse, sec

I'_{sp} theoretical specific impulse, sec

$$= \frac{1}{g}\sqrt{\frac{2k}{k-1}RT_o} = C\sqrt{\frac{T_o}{M.W.}} \qquad (A1)$$

K ratio of specific heats

M.W. molecular weight, kg/Kmol

$\dot{m}$ mass flow rate, kg/sec

P pressure, Pa

P_a arc power, W

R molar gas constant, J/Kmol K = 8315/M.W.

T_o gas temperature, K

v exhaust velocity, m/sec

η thrust efficiency

$$= \frac{\frac{1}{2}\dot{m}v_h^2}{P_a + \frac{1}{2}\dot{m}v_c^2} \qquad (A2)$$

$$= \frac{I_{sph}^2}{\frac{2}{g^2}\frac{P_a}{\dot{m}} + I_{spc}^2} \qquad (A3)$$

REFERENCES

1. Wallner, L.E.; and Czika, J., Jr.: Arcjet Thrustor for Space Propulsion. NASA TN-D-2868, 1965.

2. Todd, J.P.: 30 kW Arc-Jet Thrustor Research. APL-TDR-64-58, Giannini Scientific Corp., Mar. 1964. (AD-601534).

3. John, R.R.; Connors, J.F.; and Bennett, S.: Thirty-Day Endurance Test of a 30 kW ARC Jet Engine. AIAA Paper 63-274, June 1963.

4. The Development of an Electrothermal Propulsion System. Report no. PRE-101, Nov. 10, 1961.

5. Kallis, J.M.; Goodman, M.; and Halbach, C.R.: Viscous Effects on Biowaste Resistojet Nozzle Performance. J. Spacecr. Rockets, vol. 9, no. 12, Dec. 1972.

6. Gruber, R.P.; Private discussions. NASA Lewis Research Center, Cleveland, Ohio.

7. Zafran, S.; and Jackson, B.: Electrothermal Thruster Diagnostics, vol. II: Technical. (TRW-39152-6012-UE-00-VOL-2, TRW, Inc.; NASA Contract NAS3-23265) NASA CR-168174, 1983.

8. Hardy, T.L.: Electrode Erosion in Arc Discharge at Atmospheric Pressure. AIAA Paper 85-2018, Oct. 1985.

9. Curran, F.M.: An Experimental Study of Energy Loss Mechanisms and Efficiency Considerations in the Low Power D.C. Arcjet. AIAA Paper 85-2017, Oct. 1985.

10. Simmonds, A.L.; Miller, C.G.; and Nealy, J.E.: Tables and Charts of Equilibrium Thermodynamic Properties of Ammonia for Temperatures from 500 to 50,000 K. NASA SP-3099, 1976.

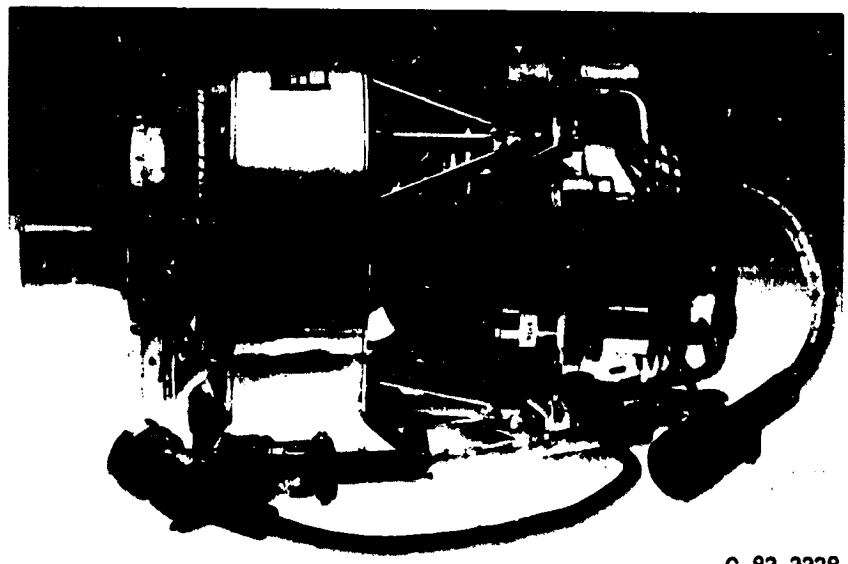

C-83-3338

Figure 1. - Plasmadyne 1 kW arcjet thruster flight system.

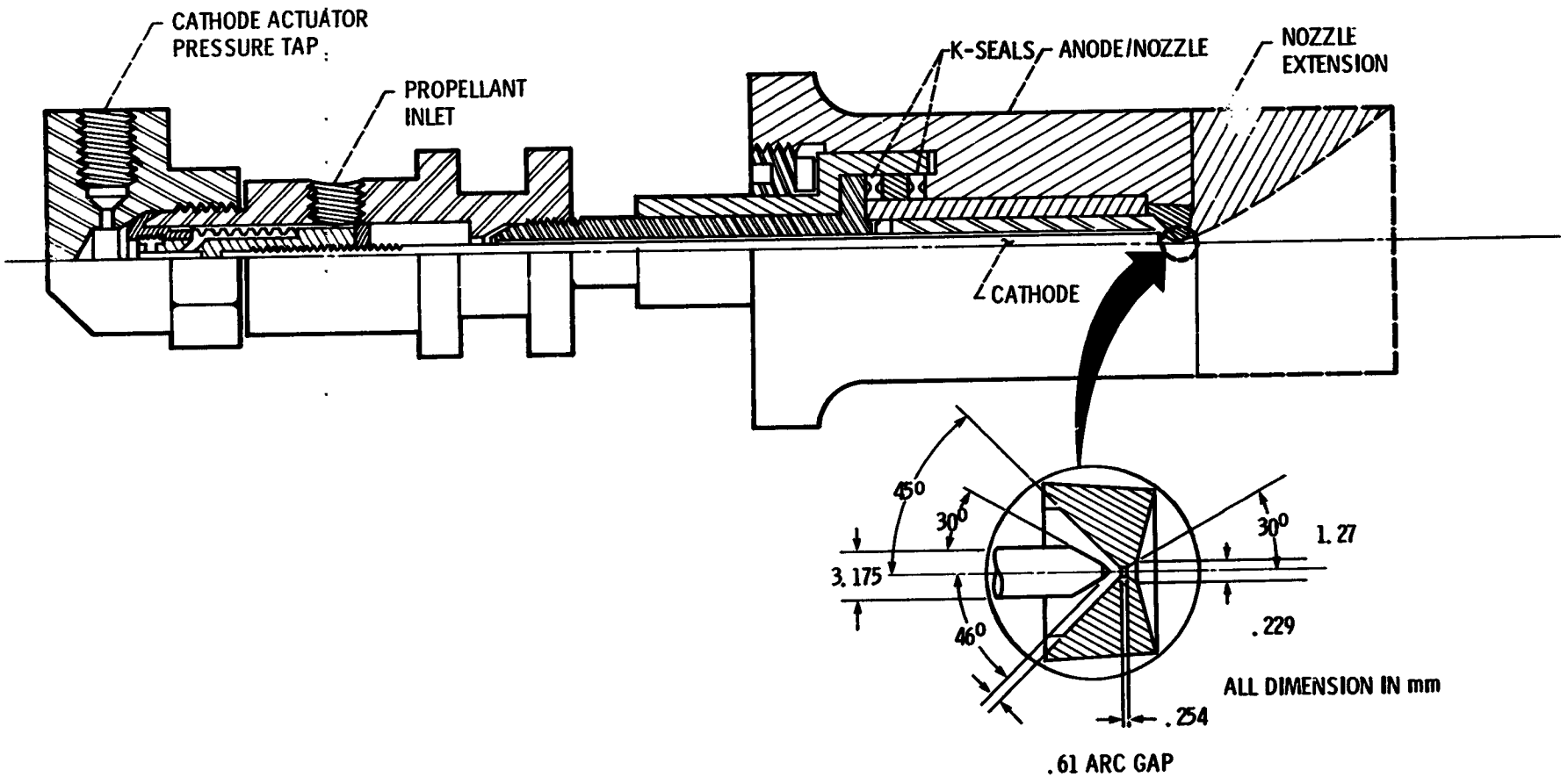

Figure 2. - Cross-section view of the cathode-anode structure and nozzle extension.

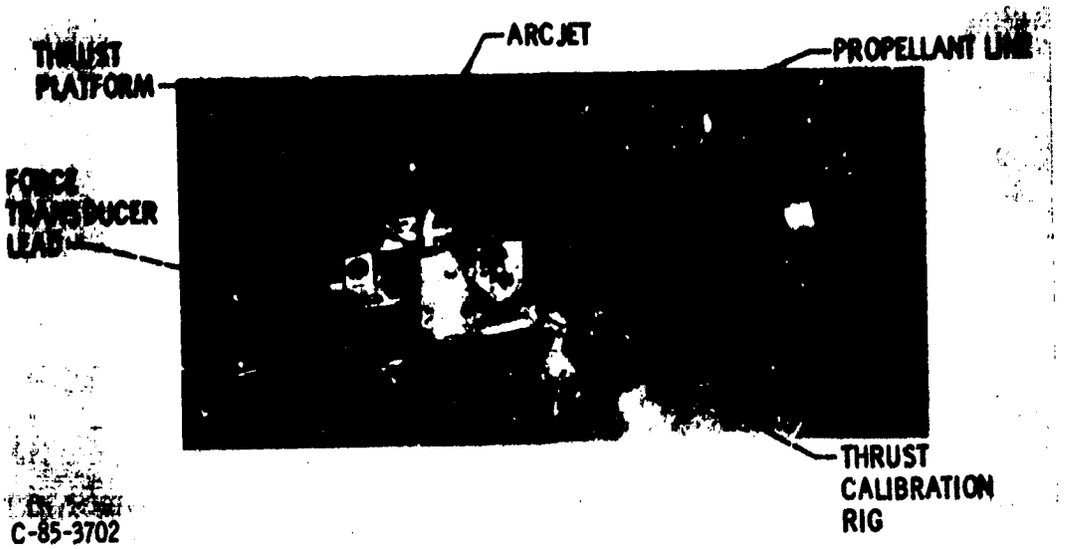

Figure 3. - Arcjet thruster mounted on thrust stand in test chamber.

Figure 4. - Photomicrograph of nozzle throat from diverging side.
Scale: 0.001 in and 0.010 in.

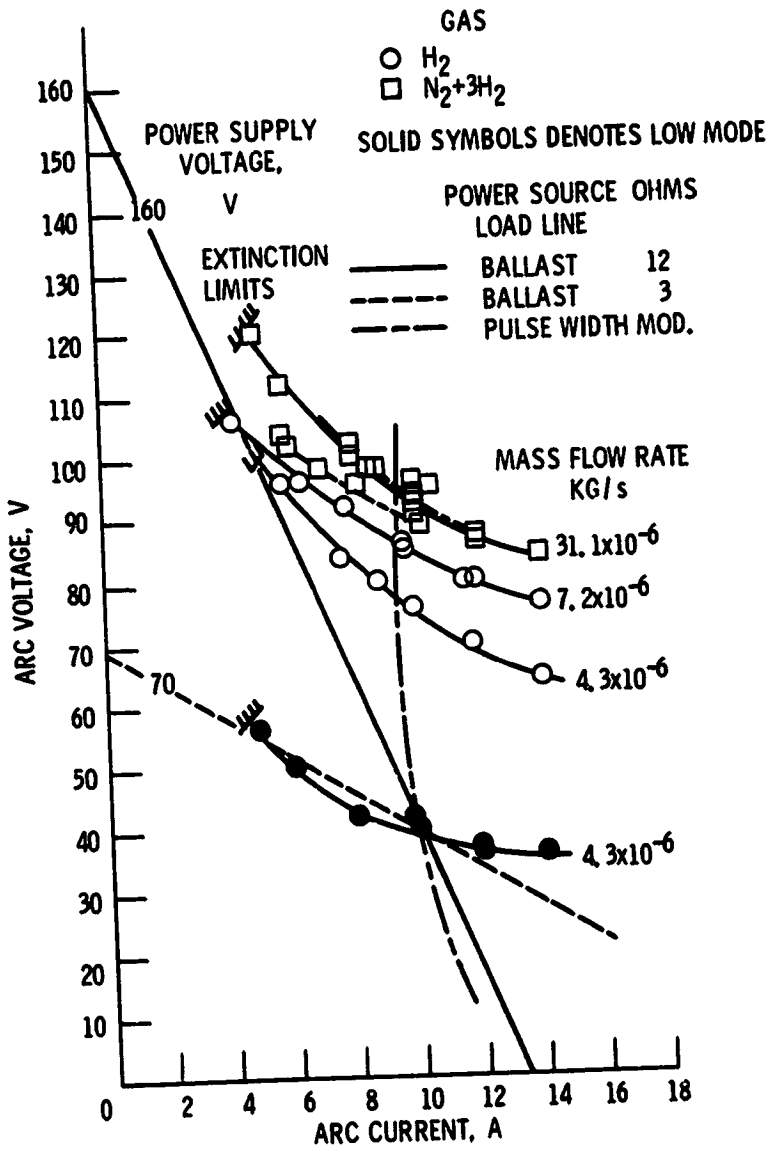

Figure 5. - Voltage - current characteristics of arc jet and power source.

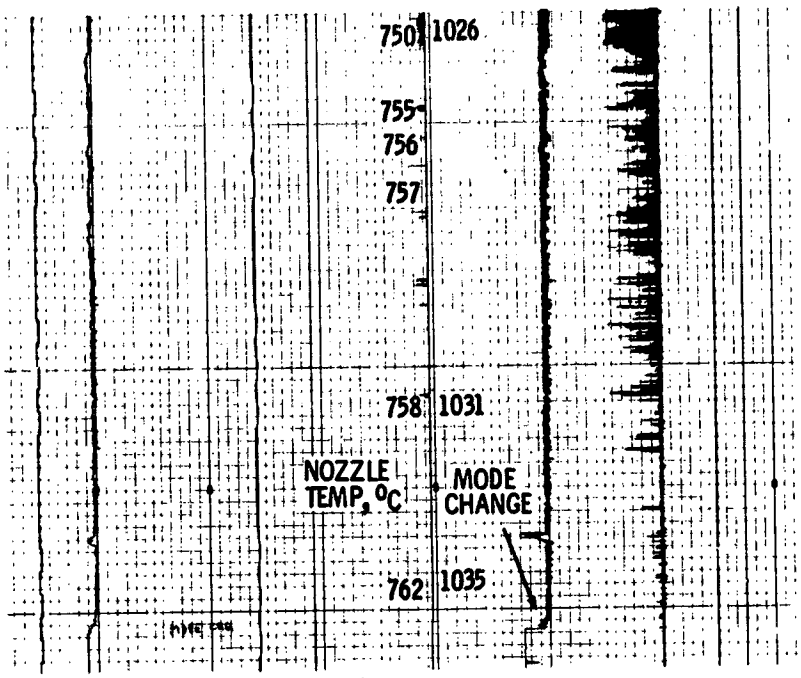

(a) Ballasted power source.

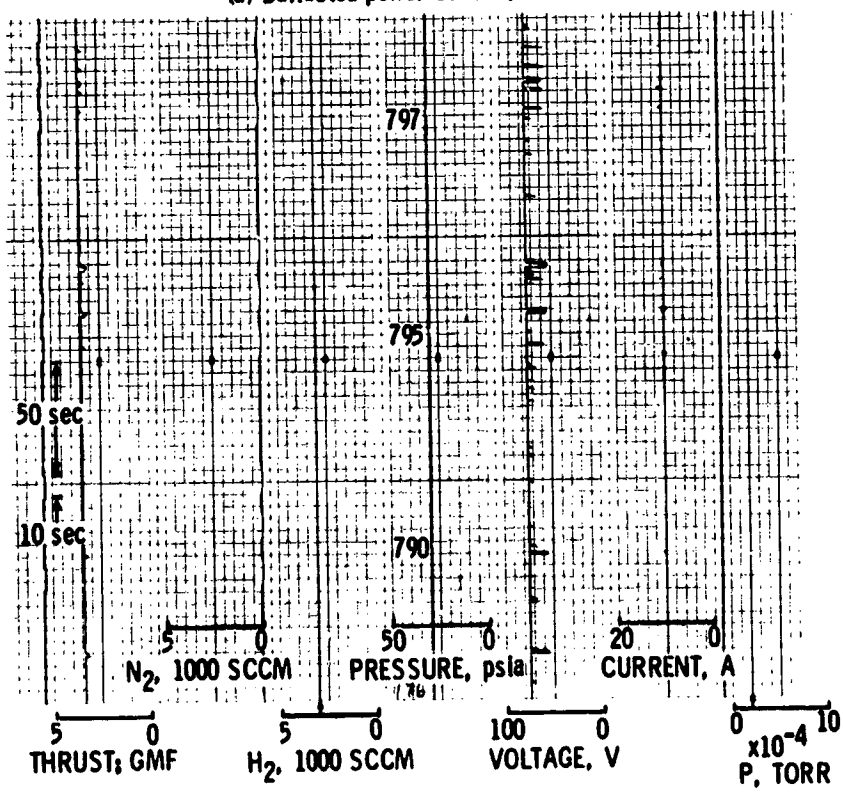

(b) Pulse-width modulated source.

Figure 6. - Transient record of arc jet operation.

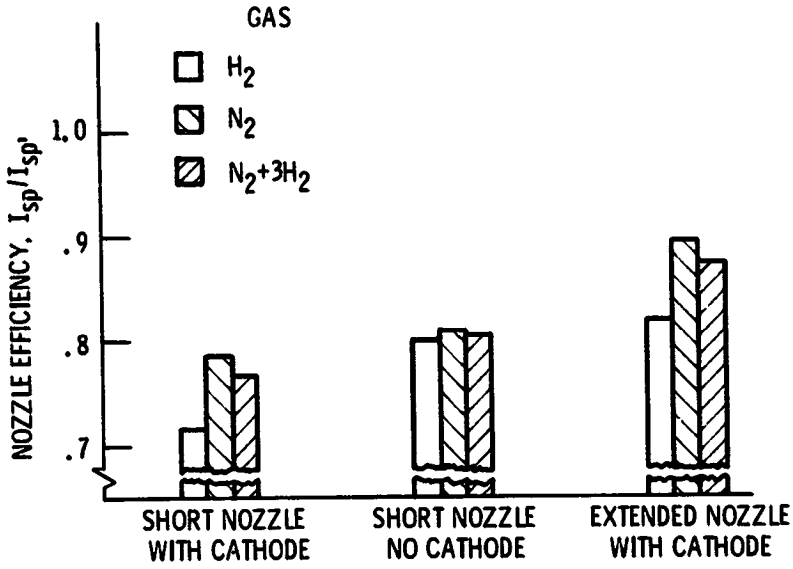

Figure 7. - Cold flow nozzle performance of various configurations and propellants. Gas temperature, 295 ^{0}K.

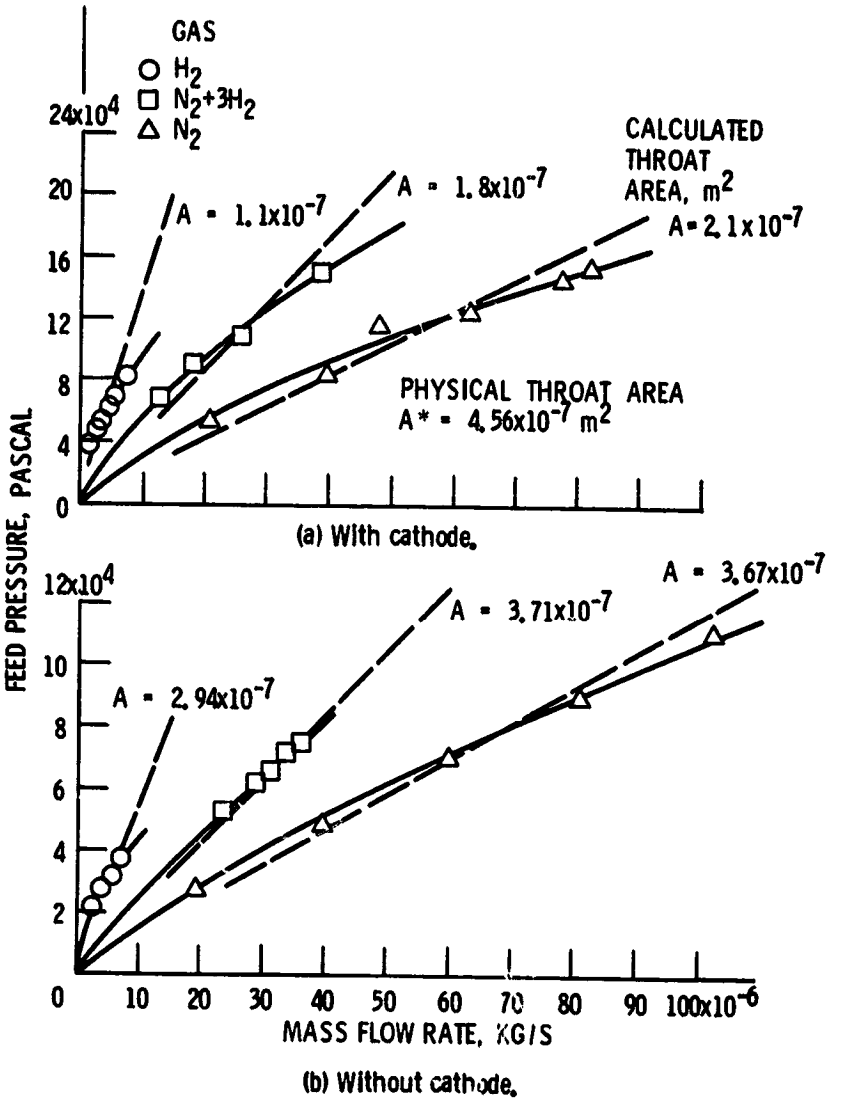

Figure 8. - Cold flow feed line pressure of the short nozzle configuration.

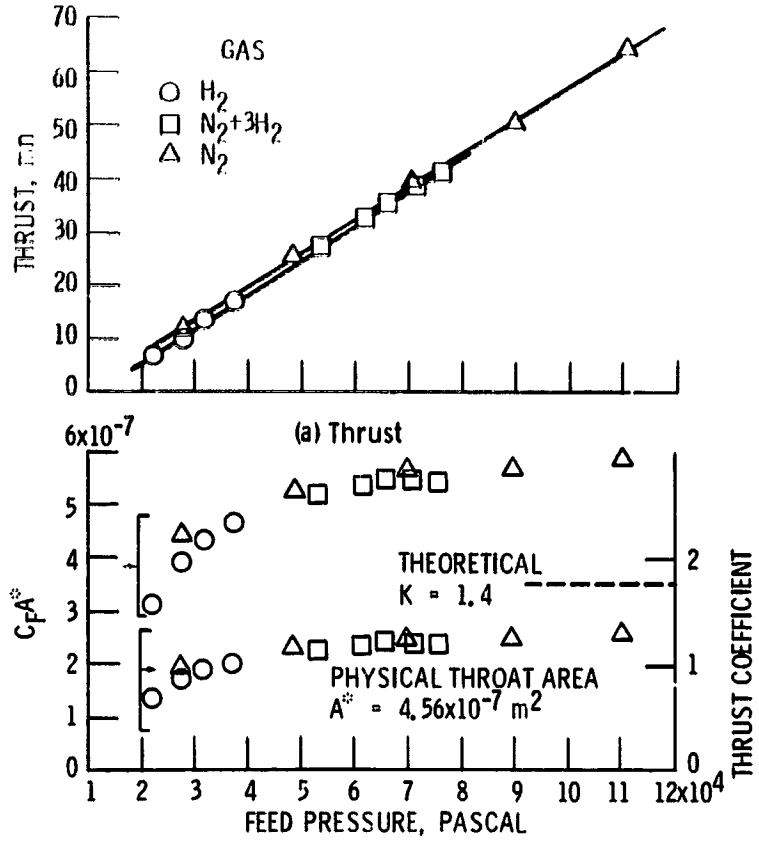

(b) Nozzle and thrust coefficients.

Figure 9. - Cold flow characteristics of short nozzle configuration without cathode.

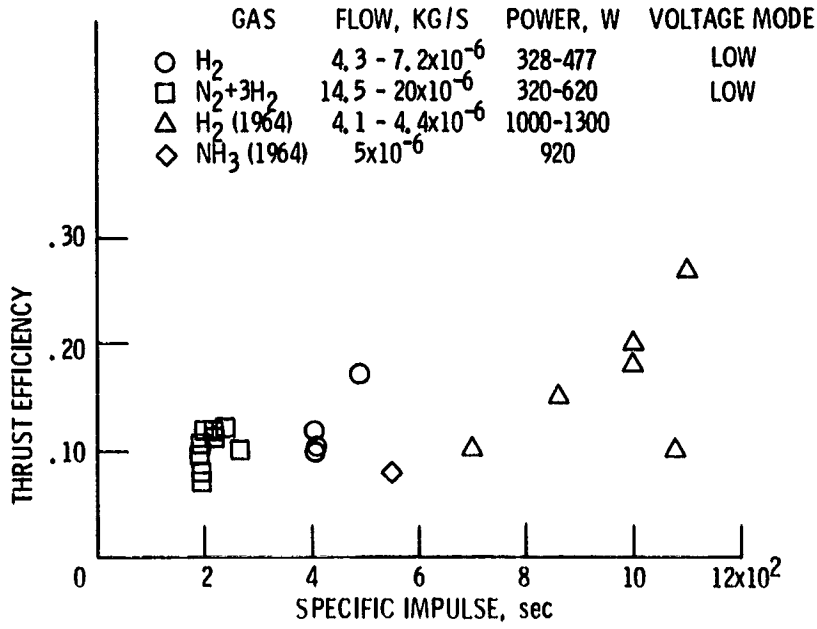

Figure 10. - Performance of short nozzle arc jet.

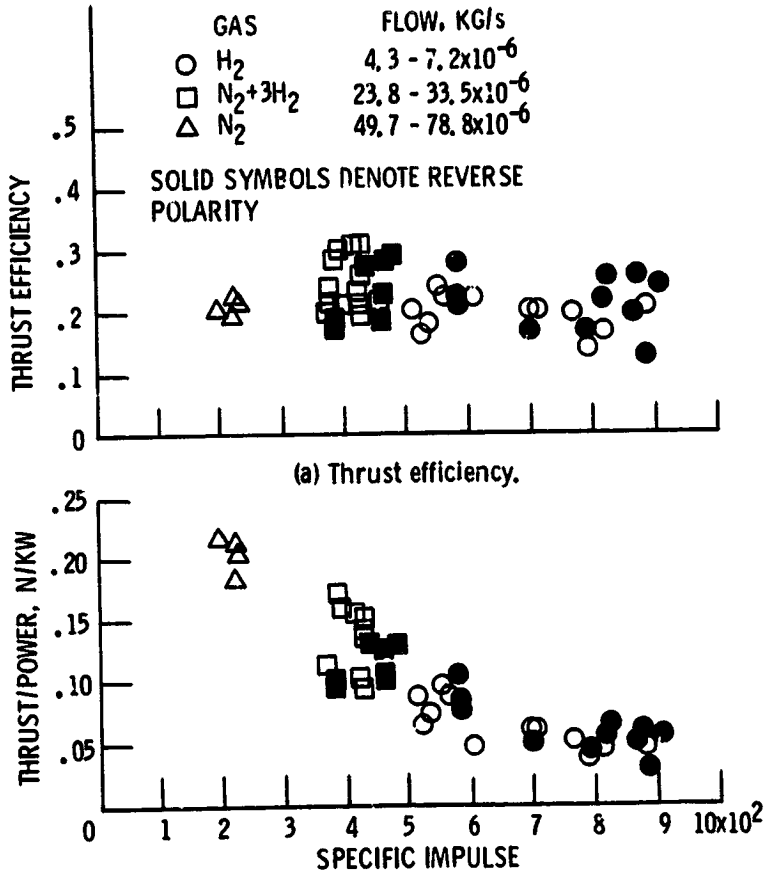

(a) Thrust efficiency.

(b) Thrust to power ratio.

Figure 11. - Performance of extended nozzle arc jet.

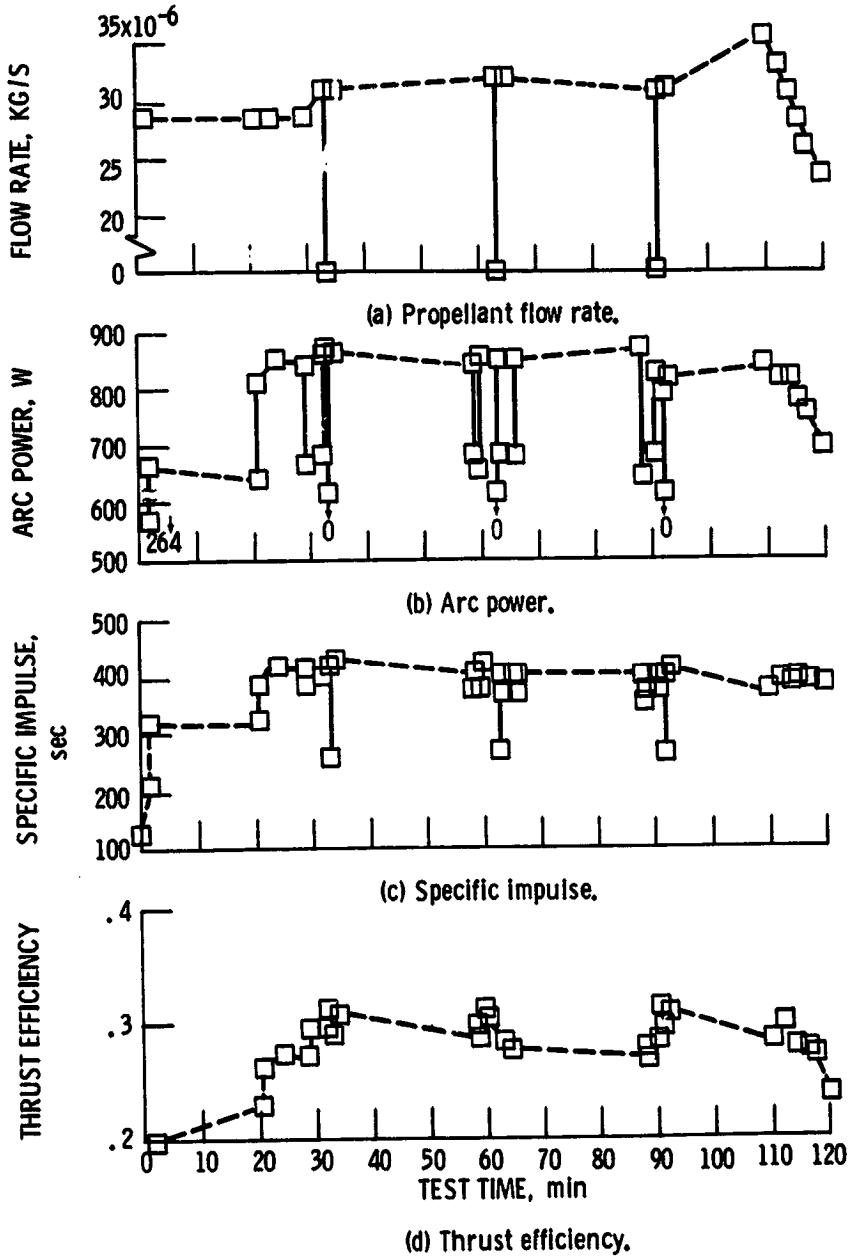

Figure 12. - Two-hour test of extended nozzle thruster using modulated power source. Propellant, N_2 + $3H_2$; arc current, 8 - 10 A.

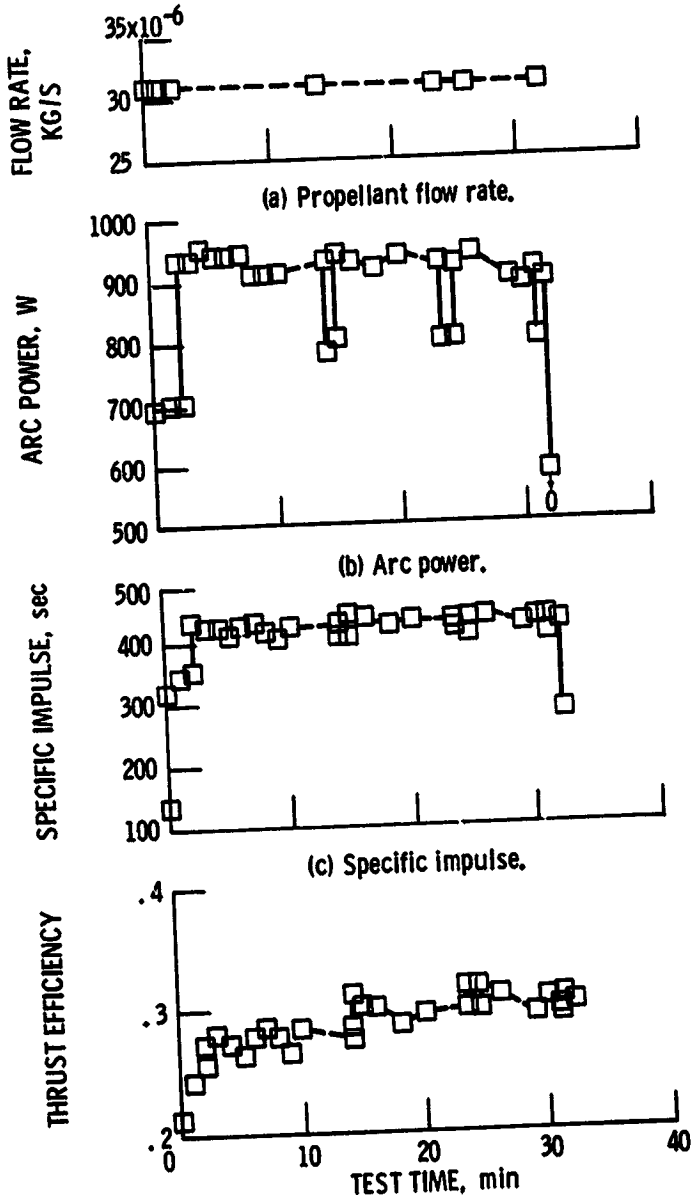

(a) Propellant flow rate.

(b) Arc power.

(c) Specific impulse.

(d) Thrust efficiency.

Figure 13. - Typical start sequence and short test of extended nozzle thruster using modulated power source. Propellant, $H_2 + {}^3H_2$; arc current, 10 A.

1. Report No.	2. Government Accession No.	3. Recipient's Catalog No.
NASA TM-87131		

4. Title and Subtitle	5. Report Date
Experimental Performance of a 1-Kilowatt Arcjet Thruster	6. Performing Organization Code: 506-55-22

7. Author(s)	8. Performing Organization Report No.
Shigeo Nakanishi	E-2744
	10. Work Unit No.

9. Performing Organization Name and Address	11. Contract or Grant No.
National Aeronautics and Space Administration Lewis Research Center Cleveland, Ohio 44135	13. Type of Report and Period Covered: Technical Memorandum

12. Sponsoring Agency Name and Address	14. Sponsoring Agency Code
National Aeronautics and Space Administration Washington, D.C. 20546	

15. Supplementary Notes

Prepared for the 18th International Electric Propulsion Conference, cosponsored by the AIAA, DGLR, and JSASS, Alexandria, Virginia, September 30-October 2, 1985.

16. Abstract

A formerly unused cathode and anode/nozzle assembly from a flight model arcjet has been tested with nitrogen, hydrogen, and nitrogen-hydrogen mixture simulating ammonia decomposition products at arc power levels from about 300 to 950 W. Two different power sources and two nozzle configurations were tested at low background pressures to exclude facility effects. Increased nozzle expansion ratio improved cold-flow nozzle efficiency from 0.8 to 0.9. Hydrogen thrust efficiency of 0.26 at 872 sec specific impulse matched some 1964 performance on a similar device. Simulated ammonia thrust efficiency was 0.31 at 422 sec. Spontaneously occurring voltage mode changes at constant arc current could be partially stabilized with appropriate power source characteristics. In the higher voltage mode specific impulse was higher, but thrust efficiency changed only slightly from that of the lower voltage mode. Sustained tests of up to 2-hr duration exhibited no apparent performance degradation with time.

17. Key Words (Suggested by Author(s))	18. Distribution Statement
Electric propulsion; Arcjet	Unclassified - unlimited STAR Category 20

19. Security Classif. (of this report)	20. Security Classif. (of this page)	21. No. of pages	22. Price*
Unclassified	Unclassified		

*For sale by the National Technical Information Service, Springfield, Virginia 22161